Adsorption of simple benzene derivatives on carbon nanotubes

L. M. Woods,[1] Ş. C. Bădescu,[2] and T. L. Reinecke[2]
[1]*Department of Physics, University of South Florida, Tampa, Florida 33620, USA*
[2]*Naval Research Laboratory, Washington, D.C. 20375, USA*
(Received 1 June 2006; revised manuscript received 27 November 2006; published 17 April 2007)

The adsorption of simple benzene derivatives composed of a benzene ring with NO_2, CH_3, or NH_2 functional groups on a semiconducting single-wall carbon nanotube is studied using the density-functional theory within the local-density approximation. The effects of molecular relaxation in the adsorption process are obtained, as well as the adsorption energies and equilibrium distances for several molecular locations and orientations on the surface. We find that all of these benzene derivatives are physisorbed mainly through the interaction of the π orbitals of the benzene ring and those of the carbon nanotube. These aromatics do not change significantly the carbon nanotube's electronic structure, and therefore only small changes in the nanotube's properties are expected. This suggests that these benzene derivatives are suitable for noncovalent nanotube functionalization and molecule immobilization on nanotube surfaces.

DOI: 10.1103/PhysRevB.75.155415 PACS number(s): 73.22.−f, 61.46.Fg, 71.15.Mb, 81.07.De

I. INTRODUCTION

Since their discovery,[1] carbon nanotubes have stimulated intense experimental and theoretical interest in their physics, chemistry, and materials science. Their unique structure and properties make them suitable for a variety of potential applications.[2] Single-wall nanotubes (SWNTs) are multifunctional materials that have potential for use as efficient gas storage elements and in battery devices, as sensors and electromechanical systems in nanoelectronics, and as biocompatible agents and sensors in medicine.[3]

The interaction of SWNTs with chemical species is the main ingredient for many of these applications. For example, it has been found experimentally and theoretically that SWNT transport properties can be changed upon exposure to O_2, H_2, NO_2, NH_3, COOH, and to some benzene compounds.[4–10] The sensitivity of SWNTs to these materials combined with their inherent characteristics such as their small size, good electrical and mechanical properties, and high surface area have led many to envision their applications in sensors and in the immobilization of biological substances, and in their use as functionalized materials.[11–16]

Aromatic compounds interacting with SWNTs are of particular interest. Noncovalent sidewall SWNT functionalization with aromatic organic molecules[11,12] has attracted increasing attention. Using SWNTs as sensors for some aromatics has also been demonstrated experimentally.[9,13] In addition, SWNT functionalization with biological molecules (such as proteins, DNA, and nucleic acids), which contain repetitions of many aromatic rings, provides potential for developing drug delivery systems, molecule immobilization, and sensors.[14] Therefore, a fundamental theoretical and systematic understanding of SWNT interaction with benzene derivatives, which appear as building blocks in large organic and biological systems, is necessary.

Cyclic aromatics consist of one or more carbon rings. The simplest example is benzene C_6H_6. The planar arrangement of its atoms creates the conditions for filling the in-plane sp^2 hybrid orbitals of C and creating a resonant bond shared by all six C atoms. Besides this aromatic bond, there is a set of π orbitals transverse to the molecular plane. Graphene itself, as well as metallic and semiconducting SWNTs, has π orbitals perpendicular to the surface.[17] Therefore, the aromatic molecules/SWNT systems can be viewed as two interacting π systems. The π-π interaction is long ranged, is relatively weak, and includes van der Waals forces. It leads to stacking, which is apparent in the interlayer bonding in graphite and in the SWNT solubilization in aromatic solvents[18] or in aromatic polymers.[19]

Benzene derivatives are obtained by substituting one or more hydrogen atoms in the benzene ring with a functional group such as hydroxil OH, methyl CH_3, nitro NO_2, or amino NH_2. The simple benzene derivatives considered here contain only one functional group. These derivatives have a common π structure from the hexagonal carbon ring, but they have distinct properties, such as permanent dipole moments and different electron affinities from the functional groups. For such aromatics, it has been observed experimentally that the electronic and transport properties of SWNTs can be modified significantly.[7,8]

In this work, the adsorption of three simple benzene derivatives on a semiconducting SWNT(8,0) is investigated using first-principles calculations based on the density-functional theory (DFT). In increasing order of electron affinity of their functional groups, these are aniline $C_6H_5NH_2$, toluene $C_6H_5CH_3$, and nitrobenzene $C_6H_5NO_2$. To understand the adsorption better, we compare the properties of these complexes with the adsorption of benzene alone, and we also compare them to the adsorption of simple closed-shell molecules without a benzene ring connected to the functional groups NH_2, CH_3, and NO_2. These molecules are amonia NH_3 (for NH_2), methane CH_4 (for CH_3), and nitromethane CH_3NO_2 (for NO_2), which are all stable under normal conditions. We also investigate the adsorption of these functional groups by themselves, trace the difference in adsorption properties mainly to whether the valence shells of the adsorbates are partially or fully filled, and discuss the contributions to the adsorption process from the π-π stacking and from the properties of the functional groups. We find that the interaction for the compounds with closed shells is always physisorption, and that in the cases with open shells,

both physisorption and chemisorption are possible.

The paper is organized as follows. In Sec. II, the method for the calculations is described. Section III gives the results from the calculations, which are discussed in Sec. IV.

II. METHOD

The results presented in this paper are obtained with self-consistent DFT calculations using the Vienna *Ab Initio* Simulation Package (VASP).[20] This state-of-the-art package uses a plane-wave basis and a periodic supercell method. It uses either ultrasoft Vanderbilt pseudopotentials or the projector-augmented wave[21] method to account for the core electrons. These methods require a relatively small number of plane waves per atom, are scalable to large systems, and are chemically accurate. For the systems studied here with full valence shells (benzene derivatives, NH_3, CH_4, and CH_3NO_2), non-spin-polarized calculations were performed. For the systems with partially filled valence shells (NH_2, CH_3, and NO_2), results from spin-polarized calculations are presented.

DFT is the most successful in describing short-ranged strong forces involving chemical bonds and large charge transfer. It gives imperfect quantitative descriptions of long-ranged, weak interactions because the local-density approximation (LDA) for the exchange-correlation functional tends to overestimate the adsorption energy and the generalized-gradient approximation (GGA) tends to underestimate it. DFT does not include dispersive forces like the van der Waals interaction.[22,23] All-electron quantum chemical calculations of the real many-body wave function including higher-order corrections to the Hartree-Fock method should give, in principle, an accurate description of van der Waals binding,[24] but this method cannot manage large molecules and large systems. Nevertheless, DFT has been found to provide a useful model for large graphitic structures, providing a distance between layers that matches the experiment. Although the formation energy of such structures is believed to be underestimated by half, DFT is successful in the correct calculation of the corrugation parallel to a graphene layer[25,26] or along a nanotube.[27] Another success is the qualitatively and quantitatively accurate description of electronic structure along the planes of graphitic structures and along the axis of carbon nanotubes; the electronic bands in these directions are mainly determined by the chemistry of sp^2 orbitals and do not depend significantly on van der Waals forces.[26,27] DFT used together with semiempirical potentials for interlayer interaction has also been reported to improve the cohesion energy of graphite, but the relative orientation and distance between graphitic layers and the electronic structure are only slightly different from the DFT results.[22,23] Therefore, due to its success in graphitic compounds, we adopt DFT here as a model for the study of the adsorption of benzene compounds on SWNTs to gain insight into their electronic structure.

We first tested the DFT method for the description of graphite. The GGA does not give a bound state of this system. The LDA gives a bound system with an in-plane lattice parameter $a_0=2.46$ Å and a vertical lattice parameter $c=6.71$ Å. These are within 0.07% and 1.3% of the experimental values, respectively.[32] The calculated binding energy is 28 meV/atom, which is higher than the energy calculated previously from semiempirical corrections to DFT.[28] Comparison with experimental data is difficult at this time due to the varying results published: measurements by Girifalco and Lad[29] give 43 meV/atom cohesive energy for graphite; experiments by Benedict *et al.*[30] show 35 meV/atom. The second test was the adsorption of benzene on a graphene surface. The GGA yields very little binding.[33] The LDA describes correctly the adsorption geometry and electronic structure, which is the most important aspect of this type of calculation. The calculated adsorption energy is almost half the experimental thermal desorption energy, which is consistent with other DFT descriptions of graphite.[31]

Next we consider the adsorption of C_6H_6, $C_6H_5NH_2$, $C_6H_5CH_3$, $C_6H_5NO_2$, NH_3, CH_4, and CH_3NO_2 on a semiconducting SWNT(8,0) within non-spin-polarized LDA. These systems all have closed valence shell structures. Spin-polarized calculations were performed for the adsorption of the open-shell functional groups NH_2, NO_2, and CH_3 on the SWNT(8,0).

The nanotube was fully relaxed before adding the adsorbates, obtaining an optimized length of a unit cell of 4.22 Å along the nanotube axis. Prior to the calculations for benzene, nitrobenzene, aniline, and toluene, three unit cells of the SWNT along the tube axis were also relaxed, obtaining a total length of 12.67 Å along the nanotube axis. For the cases of NH_3, CH_4, CH_3NO_2, NH_2, CH_3, and NO_2, a supercell with two unit cells along the tube axis was relaxed, obtaining a total length of 8.45 Å. The lateral sizes of the supercell were 21.95 Å along the adsorption direction x and 17.07 Å in the direction y. In each case, a Monkhorst-Pack k grid for sampling the Brillouin zone was taken with seven k points in the z direction and one k point in the (x,y) plane. The cutoff energy used was 420 eV. We also checked a larger E_{cutoff} parameter ($E_{cutoff}=460$ eV) in some cases, and found that the adsorption energy is slightly larger (~ 5 meV) compared to that for a smaller E_{cutoff}. The results presented here were obtained with the smaller E_{cutoff}, which assured convergence and was less demanding on computing resources.

For systems studied here, the energy convergence criterion was 10^{-5} eV, and the force convergence criterion was 0.002 eV/Å. During the adsorption calculations, the SWNT was kept frozen and the molecule was allowed to relax. In order to test the effect of nanotube relaxation during adsorption, in some cases we allowed the whole system to relax. In those cases, we found a very small variation in energy (a few meV) and essentially no difference in equilibrium orientation and relative distance between the SWNT and the molecule. For most molecules the nanotube structure was essentially unchanged, and there was no tendency toward sp^3 hybridization and pyramidalization of C atoms. The only exception was CH_3, for which relaxation of the nanotube was also allowed. The nanotube surface was distorted, indicating the appearance of sp^3 hybridization in this case.

For all molecules, the adsorption energy was obtained from

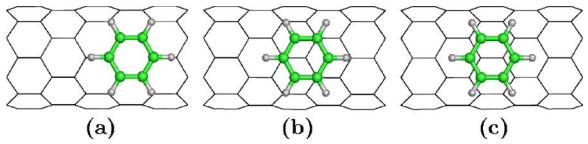

FIG. 1. (Color online) Orientations of C_6H_6 adsorbed on SWNT(8,0): (a) hollow, (b) top, and (c) bridge.

$$E_{ads} = E_{mol} + E_{SWNT} - E_{mol/SWNT}, \quad (1)$$

where E_{mol} is the energy for the relaxed molecule only, E_{SWNT} is the energy for the relaxed pristine SWNT, and $E_{mol/SWNT}$ is the energy of the molecule/SWNT complex.

III. RESULTS

A. Adsorption configurations

Several positions of the benzene carbon ring relative to the SWNT carbon rings were considered near three symmetry sites on the SWNT. Figure 1 shows these sites—bridge, top, and hollow—and the adsorption of benzene C_6H_6 on them. The adsorption of aniline, nitrobenzene, and toluene was also studied in the vicinity of the same symmetry sites, where bridge, top, and hollow refer to the location of the molecular benzene ring with respect to the SWNT carbon rings. Figure 2 shows the lowest energy configurations for these molecules: near bridge for aniline, near bridge for toluene, and near top for nitrobenzene. Other local minima are found near the other symmetry sites, as listed in Table I. This confirms previous results obtained by DFT-GGA calculations[25,35] that the adsorption of aromatics on carbon nanotubes having a surface with very shallow adhesion energy results in different local minima on the nanotube surface.

We also performed calculations for the three benzene derivatives in transverse configurations, i.e., with their functional groups pointing toward the SWNT surface and with their carbon rings situated away from the nanotube. Different configurations with the benzene plane parallel and perpendicular to the nanotube axis were considered. These correspond to interactions mainly through the functional groups, while the benzene ring has only an indirect effect on the adsorption. For all of these cases, we found that the adsorption energies are at least 150 meV smaller than when the benzene ring is parallel to the SWNT surface (Figs. 1 and 2, and Table I). This suggests that the π-π stacking is the most important ingredient in the adsorption of these aromatics, which was discussed in other works [Refs. 27 and 33–35] among which the more critical analysis in Ref. 34 showed that the π-π stacking proceeds with negligible charge transfer and hybridization. As we show in the next section for the present aromatics, our electronic structure results are in agreement with the view in Ref 34. The π-π stacking found here is also consistent with recent experiments[9] that used electric fields transverse to the nanotube axis to attach polar molecules and to modulate the capacitance of the system. Those experiments have shown that even simple dipolar aromatic molecules (with a single carbon ring) do not give a significant capacitive response compared to molecules without carbon rings, which suggests that the dipole moment of the aromatics lies flat on the surface.

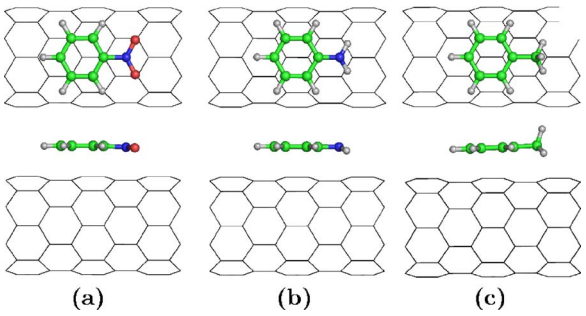

FIG. 2. (Color online) The lowest-energy configurations of simple benzene derivatives on SWNT(8,0): (a) $C_6H_5NO_2$ near the top site, (b) $C_6H_5NH_2$ near the bridge site, and (c) $C_6H_5CH_3$ near the bridge site.

In order to understand the adsorption of the different benzene derivatives well, we considered the adsorption of NH_3, CH_4, and CH_3NO_2 at the same symmetry sites. CH_3NO_2 was taken to have NO_2 toward the nanotube surface. These are

TABLE I. Benzene derivatives and simple closed-shell molecules on SWNT(8,0): adsorption energies and equilibrium distances.

	Bridge		Top		Hollow	
	E_{ads} (meV)	d (Å)	E_{ads} (meV)	d (Å)	E_{ads} (meV)	d (Å)
Benzene (C_6H_6)	260	3.12	249	3.12	151	3.22
Aniline ($C_6H_5NH_2$)	302	2.86	283	2.89	241	2.89
Toluene ($C_6H_5CH_3$)	264	2.77	259	2.77	172	2.81
Nitrobenzene ($C_6H_5NO_2$)	274	3.03	277	3.00	222	3.05
Ammonia (NH_3)	75	2.70	84	2.83	113	2.71
Methane (CH_4)	80	2.83	84	2.72	95	2.79
Nitromethane (CH_3NO_2), $x0y$	110	2.93	106	2.98	129	2.88
Nitromethane (CH_3NO_2), $x0z$	113	2.98	123	2.91	124	2.96

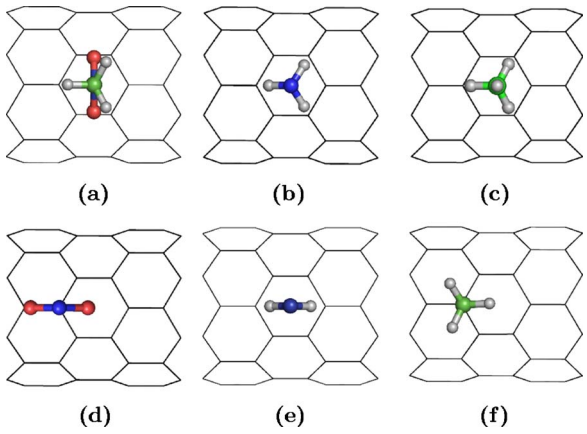

FIG. 3. (Color online) The lowest-energy configurations for simple molecules adsorbed on SWNT(8,0): (a) CH_3NO_2 near the hollow site, (b) NH_3 near the hollow site, (c) CH_4 near the hollow site, (d) NO_2 near the top site, (e) NH_2 near the hollow site, and (f) CH_3 near the top site.

closed valence shell structures containing the same functional groups as the simple aromatics, but they do not have the benzene ring. The adsorption energies and equilibrium distances are shown in Table I and Figs. 3(a)–3(c), respectively. In the lowest energy configurations, NH_3 and CH_4 have a tripod configuration, where the N and C atoms, respectively, are on the nanotube hollow site, and the H atoms point toward the neighboring C atoms from the nanotube. For CH_3NO_2, we considered only the orientations with NO_2 toward the nanotube to obtain a comparison with $C_6H_5NO_2$. In this case, we denote by $x0z$ the orientation of the symmetry plane of the NO_2 in nitromethane parallel to the nanotube axis and by $x0y$ its orientation perpendicular to the SWNT axis. The lowest energy configuration is at the hollow site in the $x0y$ configuration with O atoms pointing toward two opposite C atoms from the nanotube, as shown in Fig. 3(a).

We also calculated the adsorption energies and equilibrium distances for the three unsaturated, open-shell fragments NO_2, NH_2, and CH_3. Since these radicals have unpaired electrons, spin polarization is important and spin-polarized calculations were done here. The data for the cases in which the N atom points away from the nanotube axis are given in Table II for NO_2 and NH_2. Adsorption configurations are also possible with the N atom pointing toward the nanotube, but they have smaller energies than those with N pointing away from the tube. Again we found that bridge, top, and hollow are stable minima for both $x0y$ and $x0z$ orientations. For NO_2 we also give results from non-spin-polarized calculations to illustrate the importance of spin polarization in molecules with an open-shell electronic structure. In Figs. 3(d) and 3(e), the equilibrium configurations for NH_2 and NO_2 are shown. It can be seen that NH_2 favors the structure with N in hollow, while NO_2 prefers N on top of the C with one O atom oriented toward the bridge site and the other O oriented toward the hollow site of the nanotube.

The adsorption for CH_3 was also calculated with several starting configurations on the bridge, top, and hollow symmetry positions, with the C atom oriented away and toward the carbon nanotube with the inclusion of spin-polarization effects. All cases converged into one preferred orientation of C sitting on top of a C atom from the nanotube, as shown in Fig. 3(f). The adsorption energy was found to be 1.627 eV, and the equilibrium distance 1.54 Å.

The adsorption energies for NO_2 and NH_2 are relatively small, indicating physisorption. They are comparable to the energies for the closed-shell compounds. On the other hand, the CH_3 radical binds much more strongly to the nanotube surface via chemisorption.

There have been several reports using DFT for the adsorption on SWNTs of the small molecules considered here and also for the adsorption of benzene. For NH_3, a previous work[36] reported binding with the N atom toward the nanotube, while another work[37] found no binding. For the same molecule, other reports[38,39] find an adsorption energy of ~140 meV on a (10,0) SWNT. For CH_4 on a (10,0) SWNT, an energy of ~190 meV and a distance of 3.17 Å were obtained.[39] For NO_2, the adsorption energies obtained using non-spin-polarized[37–40] as well as spin-polarized calculations[41,42] have a rather wide range, between 300 and 600 meV. The upper value[41] suggests that stronger forces might become important. The chemical adsorption of CH_n $(n=1,2,3)$ radicals on a nanotube has also been reported previously,[43] but without spin polarization. In the case of benzene on SWNT (8,0), Tournus *et al.*[27] calculated an adsorption energy of 193 meV and a distance of 3.19 Å at the bridge site, which are 67 meV lower and 0.07 Å longer than the energy and distance found here.

We attribute the differences between the results in these reports and ours to the calculation details. Not all the previous papers include relaxation during the adsorption process. Here relaxation of the adsorbed species during the interaction process is allowed. This explains partially the difference in adsorption energy for C_6H_6/SWNT between our result and that reported by Tournus *et al.*[27] In addition, as a consequence of the long-ranged forces governing the adsorp-

TABLE II. Open-shell functional fragments on SWNT(8,0): adsorption energies and equilibrium distances.

	Bridge-$x0y$		Bridge-$x0z$		Top-$x0y$		Top-$x0z$		Hollow-$x0y$		Hollow-$x0z$	
	E_{ads} (meV)	d (Å)	E_{ads} (meV)	d (Å)	E_{ads} (meV)	d (Å)	E_{ads} (meV)	d (Å)	E_{ads} (meV)	d (Å)	E_{ads} (meV)	d (Å)
Amino (NH_2)	89	2.65	97	2.39	97	2.53	109	2.54	116	2.40	152	2.39
Nitro (NO_2), spin-pol	193	2.79	221	2.70	197	2.71	223	2.61	155	2.77	193	2.79
Nitro (NO_2), non-spin-pol	262	2.69	288	2.62	281	2.63	334	2.57	227	2.75	318	2.67

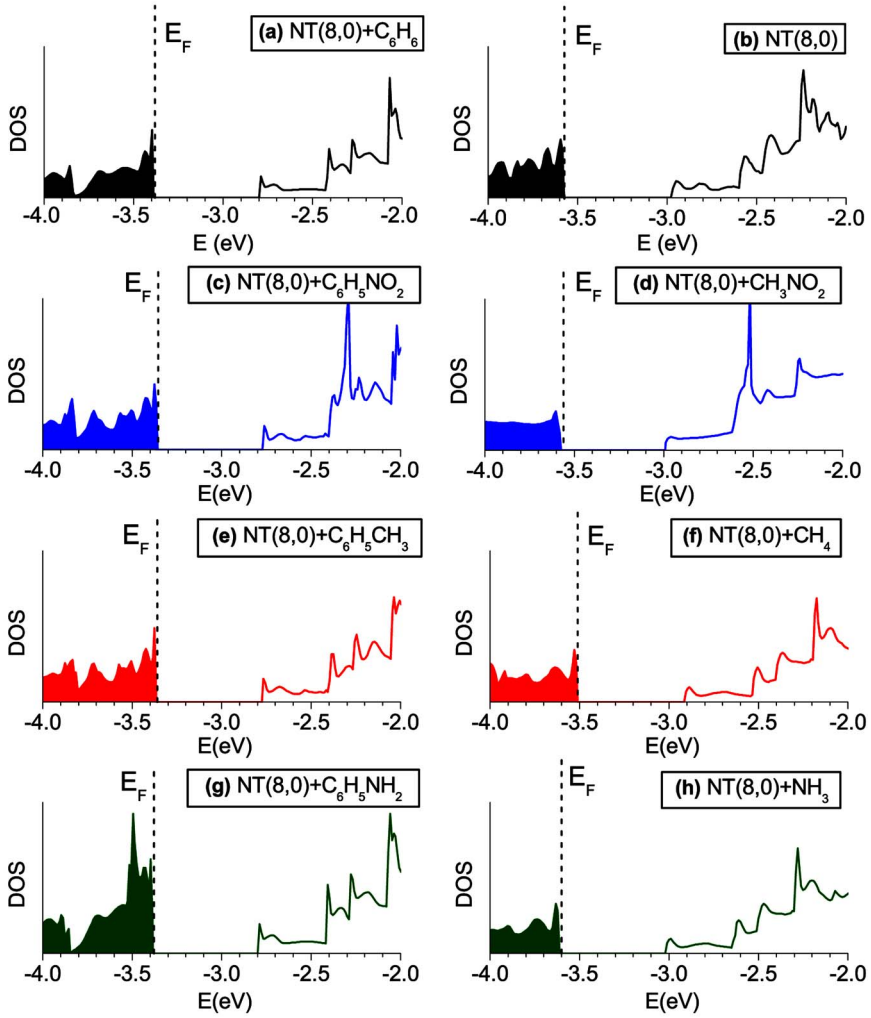

FIG. 4. (Color online) Total density of states for (a) benzene/SWNT (8,0), (b) clean/SWNT (8,0), (c) nitrobenzene/SWNT (8,0), (d) nitromethane/SWNT (8,0), (e) toluene/SWNT (8,0), (f) methane/SWNT (8,0), (g) aniline/SWNT (8,0), and (h) NH_3/SWNT (8,0).

tion, we found that the DFT-LDA results for the current molecules are sensitive to the value of the cutoff energy E_{cutoff}. A large cutoff parameter must be used to include many plane waves in the calculation, as described earlier by Girifalco and Hodat [23] for graphite. Using a small cutoff parameter may result in unphysically large adsorption energies. We performed calculations for NO_2 with E_{cutoff}=420 eV and also with E_{cutoff}=320 eV. The adsorption energy for the smaller E_{cutoff} was E_{ads}=550 meV, which is in the range found in the literature.[41]

A comparison of equilibrium distances for the four aromatics studied here shows that the distance between benzene and the SWNT surface is the largest. The distances for the benzene derivatives are all shorter than the distance of 3.12 Å for benzene (Table I). Also, the adsorption energies for the benzene derivatives studied here are larger than the adsorption energy for benzene, with E_{ads} for toluene just slightly above that for benzene (Table I), and they are also larger than the E_{ads} for the functional groups (when spin-polarization effects are included for NO_2). All adsorption energies for these aromatics are in the physisorption range. To determine the relative contribution to the adsorption of benzene and its functional groups, we now look in detail at the electronic structures of the different systems.

B. Electronic structure

Here we give results for the electronic structure of the benzene derivatives as well as of their building blocks. Figure 4 shows the total electronic density of states (DOS) for the benzene derivatives studied here and for the small closed-shell molecules that contain the same functional groups. The DOS for the pristine semiconducting SWNT(8,0) is given as a reference in Fig. 4(b).

First we consider the adsorption of benzene, which is the simplest aromatic structure. Benzene has enhanced stability attributed to its delocalized π electronic structure and its closed-shell structure. It has very little effect on the total density of states near the SWNT band gap [Fig. 4(a)]. The molecule's highest occupied molecular orbital (HOMO) is deep in the nanotube valence band, and its lowest unocoupied molecular orbital (LUMO) is high in the conduction band. Only the states for benzene that are about 2 eV below the gap are somewhat perturbed, so the band gap of the SWNT changed little. Mulliken analysis shows a very small charge rearrangement in the region between the molecule and the nanotube ($<0.01\ e$), which is within the accuracy limit of the method used.

Although $C_6H_5NO_2$ is a charge acceptor due to the electronegativity of NO_2, no charge transfer is found for the

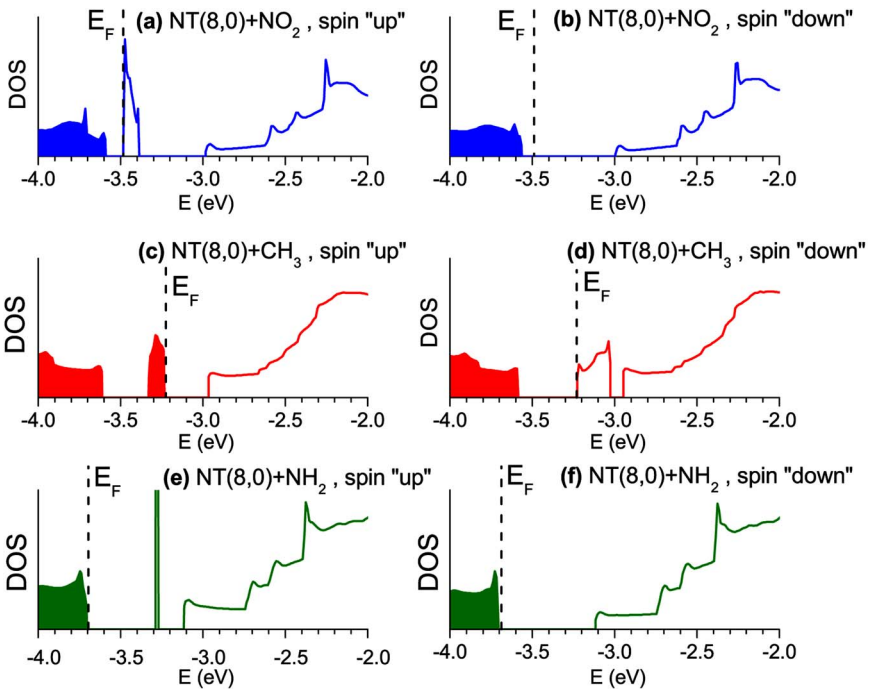

FIG. 5. (Color online) Total density of states from spin-polarized calculations for (a) NO_2/SWNT(8,0), spin up; (b) NO_2/SWNT(8,0), spin down; (c) CH_3/SWNT(8,0), spin up; (d) CH_3/SWNT(8,0), spin down; (e) NH_2/SWNT(8,0), spin up; and (f) NH_2/SWNT(8,0), spin up.

nitrobenzene/SWNT. The HOMO of nitrobenzene is deeper in energy than the HOMO of NO_2, and it is completely filled. Figure 4(c) for $C_6H_5NO_2$/SWNT shows a perturbation of the total DOS at about 1.5 eV above the band gap due to the LUMO of the molecule. Otherwise, there is little effect around the band gap and Fermi level from the NO_2 functional group. If a stronger hybridization were to take place, one would expect that the equilibrium configuration of the molecule would be closer to the transverse direction due to a stronger attraction of the NO_2 to the SWNT. This was not observed here.

For the toluene adsorption, it is evident from Fig. 4(e) that the semiconducting nature of the SWNT is also preserved and that the energy gap changed very little. We notice that the profile of the total DOS is very similar to that for C_6H_6/SWNT. This is consistent with the adsorption energy (Table I) being close to that for benzene and to the fact that CH_3 has little electronegativity. No charge transfer is found between the toluene and the SWNT, and the adsorption results primarily from the π-π interaction.

Aniline is expected to be a charge donor because NH_2 is electropositive. Here a small charge redistribution is found between this molecule and the SWNT. Figure 4(g) indicates that there are no other hybrid states in the semiconducting gap. However, a different hybrid state appears below the top of the valence band but does not affect the Fermi level. A decomposition of the DOS indicates that the state is formed due to hybridization between the highest SWNT valence band and the aniline HOMO and that it is mainly of p character.

In order to understand better the adsorption of the benzene derivatives on nanotubes, we now analyze the electronic structure of the different functional groups themselves. We recognize that the unsaturated functional groups have a qualitatively different electronic shell structure than when they are saturated by attaching to C_6H_5 (from the benzene ring) or other fragments. The functional groups NO_2, NH_2, and CH_3 considered here all have a partially filled valence electron shell. When they are substituted for a H atom in benzene, the resulting complex has a filled valence shell. Thus the functional groups will adsorb differently on the nanotube surface if they are attached to a benzene ring than when they are unsaturated. To clarify this issue, we studied the adsorption of simple closed-shell molecules that contain the functional groups. Then we describe the open-shell fragments themselves.

In Figs. 4(d), 4(f), and 4(h), the total DOS is given for nitromethane CH_3NO_2, methane CH_4, and amonia NH_3. It can be seen that the adsorption of these molecules also has little effect on the density of states of the clean nanotube around the SWNT band gap. The compounds have a HOMO and a LUMO far in the valence and conduction bands of the SWNT(8,0), respectively. In addition, their closed-shell structure makes them unreactive to other compounds in a similar manner as the closed-shell benzene derivatives. In summary, we found that all closed valence shell adsorbates examined here adsorb weakly and do not change the nanotube electronic structure significantly.

The total density of states for the partially filled valence shell fragments NH_2, NO_2, and CH_3 are given in Fig. 5. Their behavior is different from the closed-shell systems. For these systems, spin-polarized calculations have been done. The HOMO of NO_2 is close to the valence-band edge of the SWNT and is partially filled. After the adsorption, this state is hybridized with the highest conduction states of the nanotube and stays under the band gap. Also a peak appears right above the Fermi level for "spin up." This state is empty and contains little admixture from the C orbitals. No such state is found for "spin down." The Mulliken analysis shows that there is very little charge transfer in the system $\sim$0.01 e. For NH_2 we also found a peak mainly of p character from the fragment 400 meV above the Fermi level for spin up, which

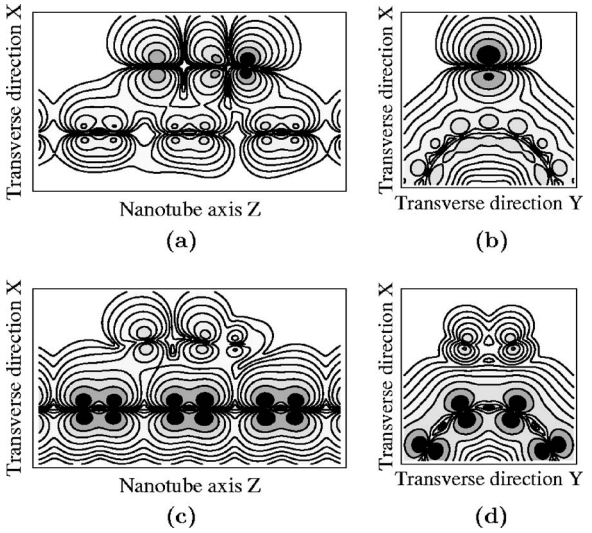

FIG. 6. Plots of charge density in five subbands at the top of the valence bands for [(a) and (b)] $C_6H_5NH_2$/SWNT(8,0) and [(c) and (d)] $C_6H_5NO_2$/SWNT(8,0). In each figure the dark areas represent the highest densities. The contour plots are on a logarithmic scale. (a) and (c) show plots for the SWNT axial cuts; (b) and (d) show plots for cuts perpendicular to the SWNT axis through the functional atoms H for aniline and O for nitrobenzene.

is also an empty state. No such peak is obtained for spin down.

For CH_3, the spin-polarization calculations result in spin-up states right under the Fermi level that are completely filled and in spin-down states that are empty. These states result from a strong hybridization between the CH_3 and the nanotube. This bond is of sp^3 character and is a result of the admixture between the C states from the radical and the C states from the four atoms from the nanotube under the CH_3. We also found that there is a deformation of the nanotube surface under the radical upon its adsorption, which is a manifestation of the sp^3 bonding. Mulliken analysis estimates that there is a charge transfer of 0.2 e toward the molecule. For the case of CH_3, we obtain stronger bonding, more hybridization, and more nanotube deformation than for the other adsorbates studied here. This results from the strong C-C bond formed with the carbon nanotube.

Further insight can be gained from charge-density contour plots of the electronic densities. They were obtained with the LEV00 computer code.[44] In Fig. 6 we present contour plots for $C_6H_5NO_2$ and $C_6H_5NH_2$. For nitrobenzene/SWNT, the charge density is simply a superposition of the charge densities for the molecule and the SWNT separately, and very little hybridization occurs. Nitrobenzene sits on the top site and interferes little with the SWNT electronic structure. For aniline/SWNT, hybridization occurs between the highest valence bands just below the SWNT gap and the aniline HOMO. The π bonds of the C atoms from the nanotube are somewhat distorted and are hybridized with the N levels from aniline. The H atoms from the NH_2 functional group from aniline do not affect the SWNT; the hybridization occurs mainly with the N atom.

Figure 7 shows total charge-density plots for the axial and transverse nanotube directions for the spin-polarized calculations for NO_2/SWNT and CH_3/SWNT. For the NO_2 case, the states above the Fermi level have very little admixture from the nanotube, and thus no charge transfer between the NO_2 and nanotube orbitals occurs. For CH_3, strong sp^3 hybridization of the C atom with nanotube states occurs, resulting in a significant charge transfer in the system.

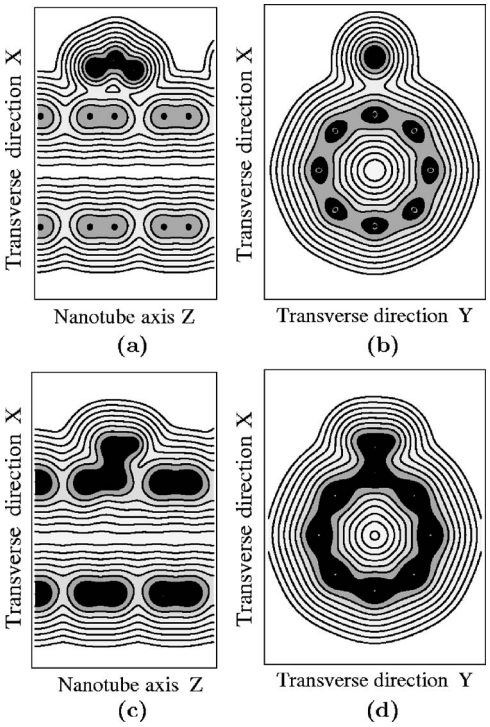

FIG. 7. Total charge-density plots for [(a) and (b)] NO_2/SWNT(8,0) and [(c) and (d)] CH_3/SWNT(8,0). The contour plots are on a logarithmic scale. In each figure the areas with the largest density are represented by dark gray. (a) and (c) show plots for the SWNT axial cuts; (b) and (d) show plots for cuts perpendicular to the SWNT axis through the functional atoms N and C.

IV. CONCLUSIONS

The present results from the DFT calculations can be used to determine the important physical features in the adsorption process of benzene derivatives on SWNTs. One factor is that the noncovalent π-π interaction between the benzene ring and the nanotube is the dominant adsorption mechanism regardless of the charge-transfer properties of the functional groups or the locations of their electronic states with respect to the nanotube gap. The functional groups have only a secondary effect on the adsorption and have small effects on the electronic properties of the semiconducting SWNT. The calculated binding energies and equilibrium distances are consistent with physisorption.

In the case of the adsorption of the open-shell functional fragments studied here, the existence of a partially filled orbital and the position of the HOMO-LUMO with respect to the nanotube gap are also other important factors in the nanotube adsorption. We see that for simple closed-shell molecules similar to the open-shell fragments, the adsorption is similar to that for the benzene derivatives. On the other

hand, the adsorption of the open-shell fragments themselves can change the nanotube electronic structure significantly.

The comparison of the equilibrium distances and energies for the different adsorbed aromatic molecules suggests some competition between the benzene ring and the functional groups. The equilibrium distances for the benzene derivatives are smaller than those for C_6H_6 and greater than those for the respective functional groups, with the exception of toluene (Table I). Also, the adsorption energies for the benzene-derived aromatics are larger than the adsorption energy for benzene, indicating that functional groups affect the adsorption process to some extent. Again, the exception is toluene, for which the energy is very close to that for benzene (Table I). The carbon ring of benzene tends to keep the molecule at a distance characteristic of π-π stacking in graphitic structures, whereas the functional group tends to bring the molecule closer to the SWNT.

These results suggest that these benzene derivatives can be used for the noncovalent functionalization of carbon nanotubes. These aromatics might also play a role in systems for biological species immobilization on nanotubes. Our results for the adsorption of open-shell systems might be important for the chemical functionalization of carbon nanotubes.

ACKNOWLEDGMENTS

We acknowledge stimulating discussions with E. S. Snow. We also acknowledge the services of the High Performance Computing facilities of the DoD and the services of the Research Computing Core at the University of South Florida. S.C.B. acknowledges support from NRL-NRC during part of this work. L.M.W. acknowledges partial support from the University of South Florida and from the Petroleum Research Fund, administered by the American Chemical Society.

[1] S. Iijima, Nature (London) **354**, 56 (1991).
[2] M. S. Dresselhaus, G. Dresselhaus, and P. C. Eklund, *Science of Fullerenes and Carbon Nanotubes* (Academic, New York, 1996).
[3] M. S. Dresselhaus, G. Dresselhaus, and P. Avouris, *Carbon Nanotubes: Synthesis, Structure, Properties and Applications* (Springer, Berlin, 2000).
[4] P. G. Collins, K. Bradley, M. Ishigami, and Z. Zettl, Science **287**, 1801 (2000); K. Bradley, S. H. Jhi, P. G. Collins, J. Hone, M. L. Cohen, S. G. Louie, and A. Zettl, Phys. Rev. Lett. **85**, 4361 (2000).
[5] A. C. Dillon, K. M. Jones, T. A. Bekkedahl, C. H Kiang, D. S. Bethune, and M. J. Hebe, Nature (London) **386**, 377 (1997); Y. Ye, C. C. Ahn, C. Withman, B. Fultz, J. Liu, A. G. Rinzler, D. Colbert, K. A. Smith, and R. E. Smalley, Appl. Phys. Lett. **74**, 2307 (1999).
[6] J. Kong, N. R. Franklin, C. Zhou, M. G. Chapline, S. Peng, K. Cho, and H. Dai, Science **287**, 622 (2000).
[7] G. U. Sumanasekera, B. K. Pradhan, H. E. Romero, K. W. Adu, and P. C. Eklund, Phys. Rev. Lett. **89**, 166801 (2002).
[8] A. Star, T. R. Han, J. C. P. Gabriel, K. Bradley, and G. Gruener, Nano Lett. **3**, 1421 (2003); J. Zhang, J. K. Lee, Y. Wu, and R. W. Murray, *ibid.* **3**, 403 (2003).
[9] E. S. Snow, F. K. Perkins, E. J. Houser, Ş. C. Bădescu, and T. L. Reinecke, Science **307**, 1942 (2005).
[10] H. Park, J. Zhao, and J. P. Lu, Nano Lett. **6**, 916 (2006).
[11] R. J. Chen, Y. Zhang, D. Wang, and H. J. Dai, J. Am. Chem. Soc. **123**, 3838 (2001).
[12] X. Wang, Y. Liu, W. Qiu, and D. Zhu, J. Mater. Chem. **12**, 1636 (2002).
[13] M. Penza, F. Antolini, and M. V. Antisari, Sens. Actuators B **100**, 47 (2004).
[14] H. Gao and Y. Kong, Annu. Rev. Mater. Res. **34**, 123 (2004).
[15] S. Chopra, K. McGuire, N. Gothard, A. M. Rao, and A. Pham, Appl. Phys. Lett. **83**, 2280 (2003).
[16] M. J. Moghaddam, S. Taylor, M. Gao, S. Huang, L. Dai, and M. J. McCall, Nano Lett. **4**, 89 (2004).
[17] E. Joselevich, ChemPhysChem **5**, 619 (2004).
[18] Y. Sun, S. R. Wilson, and D. I. Schuster, J. Am. Chem. Soc. **123**, 5348 (2001).
[19] A. Star, Y. Liu, K. Grant, L. Ridvan, J. F. Stoddart, D. W. Steuerman, M. R. Diehl, A. Boukai, and J. R. Heath, Macromolecules **36**, 553 (2003).
[20] G. Kresse and J. Furthmller, *VASP the GUIDE*, http://cms.mpi.univie.ac.at/vasp/vasp/vasp.html
[21] G. Kresse and D. Joubert, Phys. Rev. B **59**, 1758 (1999).
[22] H. Rydberg, M. Dion, N. Jacobson, E. Schroder, P. Hyldgaard, S. I. Simak, D. C. Langreth, and B. I. Lundqvist, Phys. Rev. Lett. **91**, 126402 (2003).
[23] L. A. Girifalco and M. Hodak, Phys. Rev. B **65**, 125404 (2002).
[24] M. A. Sinnokrot, E. F. Valeev, and C. D. Sherill, J. Am. Chem. Soc. **124**, 10887 (2002).
[25] A. N. Kolmogorov and V. H. Crespi, Phys. Rev. B **71**, 235415 (2005).
[26] J. C. Charlier, X. Gonze, and J. P. Michenaud, Europhys. Lett. **28**, 403 (1994).
[27] F. Tournus and J. C. Charlier, Phys. Rev. B **71**, 165421 (2005); F. Tournus, S. Latil, M. I. Heggie, and J. C. Charlier, *ibid.* **72**, 075431 (2005).
[28] F. Ortmann, F. Bechstedt, and W. G. Schmidt, Phys. Rev. B **73**, 205101 (2006).
[29] L. A. Girifalco and R. A. Lad, J. Chem. Phys. **25**, 693 (1956).
[30] L. X. Benedict, N. C. Chopra, M. L. Cohen, A. Zettl, S. G. Louie, and V. C. Crespi, Chem. Phys. Lett. **286**, 490 (1998).
[31] R. Zacharia, H. Ulbricht, and T. Hertel, Phys. Rev. B **69**, 155406 (2004).
[32] Y. Baskin and L. Meyer, Phys. Rev. **100**, 544 (1955).
[33] J. Zhao, J. P. Lu, J. Han, and C. K. Yang, Appl. Phys. Lett. **82**, 3746 (2003).
[34] P. Gianozzi, Appl. Phys. Lett. **84**, 3936 (2004).
[35] D. L. Irving, S. B. Sinnott, and A. S. Lindner, Chem. Phys. Lett. **389**, 96 (2004).

[36] H. Chang, J. D. Lee, S. M. Lee, and Y. H. Lee, Appl. Phys. Lett. **79**, 3863 (2001).
[37] S. Peng and K. Cho, Nanotechnology **11**, 57 (2000).
[38] J. Lu, S. Nagase, Y. Maeda, T. Wakahara, T. Nakado, T. Akasaka, D. Yu, Z. Gao, R. Han, and H. Ye, Chem. Phys. Lett. **405**, 90 (2005).
[39] J. Zhao, A. Buldum, J. Han, and J. P. Lu, Nanotechnology **13**, 195 (2002).
[40] W. L. Yim, X. G. Gong, and Z. F. Liu, J. Phys. Chem. B **107**, 9363 (2003).
[41] S. Peng, K. Cho, P. Qi, and H. Dai, Chem. Phys. Lett. **387**, 271 (2004).
[42] S. Santucci, P. Picozzi, F. D. Gregorio, L. Lozzi, C. Cantalini, L. Valentini, J. M. Kenny, and B. Delley, J. Chem. Phys. **119**, 10904 (2003).
[43] F. Li, Y. Xia, M. Zhao, X. Liu, B. Huang, Z. Tan, and Y. Ji, Phys. Rev. B **69**, 165415 (2004).
[44] L. N. Kantorovich, *User-friendly Visualisation Program for Ab Initio DFT Codes VASP and SIESTA*, 1996–2005, www.cmmp.ucl.ac.uk/~lev/codes/lev00